MycoKeys 110: 93–115 (2024)
DOI: 10.3897/mycokeys.110.135538

Research Article

Ophiostomatalean fungi associated with *Polygraphus* bark beetles in the Qinghai-Tibet Plateau, China

Zheng Wang[1], Caixia Liu[2], Xiuyue Song[1], Yingjie Tie[1], Huimin Wang[2], Huixiang Liu[1], Quan Lu[2]

1 *Shandong Research Center for Forestry Harmful Biological Control Engineering and Technology, College of Plant Protection, Shandong Agricultural University, Tai'an 271018, China*

2 *Key Laboratory of Forest Protection of National Forestry and Grassland Administration, Ecology and Nature Conservation Institute, Chinese Academy of Forestry, Beijing 100091, China*

Corresponding author: Quan Lu (luquan@caf.ac.cn)

Abstract

Climate change has exacerbated outbreaks of forest pests worldwide. In recent years, bark beetles have caused significant damage to coniferous forests of the Northern Hemisphere. *Polygraphus* bark beetles are widely distributed secondary pests. Recently, tree mortality caused by these beetles on the Qinghai-Tibet Plateau has been increasing; however, few studies have focused on their fungal associations. In the present study, we explored the diversity of ophiostomatalean fungi associated with these beetles on the north-eastern and southern Qinghai-Tibet Plateau. We isolated 442 ophiostomatalean strains from adult beetles and their fresh galleries, specifically targeting *Polygraphus poligraphus* and *Polygraphus rudis* infesting *Picea crassifolia* and/or *Pinus griffithii*. Based on phylogenetic and morphological features, we assigned the 442 strains to 16 species belonging to *Grosmannia* spp., *Leptographium* spp. and *Ophiostoma* spp. Amongst these, *Ophiostoma maixiuense* and *Ophiostoma bicolor* were the most frequently isolated species, accounting for 20.8% and 18.1% of the total number of ophiostomatalean assemblages, respectively. By comparing their fungal communities, we found that the different patterns of fungal assemblages of bark beetles from the north-eastern and southern Qinghai-Tibet Plateau may be influenced by biogeographic barriers and host tree species. The results of this study enhance our understanding of bark beetle fungal assemblages, especially *Polygraphus*, on the Qinghai–Tibet Plateau, with implications for forest management under changing climate.

Key words: Conifer, forest pest, *Grosmannia*, *Leptographium*, *Ophiostoma*, pine, spruce, symbiosis

OPEN ACCESS

Academic editor: Xinlei Fan
Received: 26 August 2024
Accepted: 8 October 2024
Published: 1 November 2024

Citation: Wang Z, Liu C, Song X, Tie Y, Wang H, Liu H, Lu Q (2024) Ophiostomatalean fungi associated with *Polygraphus* bark beetles in the Qinghai-Tibet Plateau, China. MycoKeys 110: 93–115. https://doi.org/10.3897/mycokeys.110.135538

Introduction

Extreme heat and frequent droughts driven by climate change have exacerbated forest pest outbreaks (Biedermann et al. 2019). Recently, bark beetles have inflicted severe damage on coniferous forests across the Northern Hemisphere. In Europe, *Ips typographus* continues to devastate spruce forests, while the frequency of *Ips acuminatus* outbreaks has increased, leading to significant pine tree mortality (Popkin 2021; Papek et al. 2024). A similar trend has been

observed in North America, where elevated temperatures have removed climatic barriers, enabling the northward spread of the aggressive beetles *Dendroctonus frontalis* and *Dendroctonus ponderosae*, which now threaten additional pine forest species and regions (Bentz and Jönsson 2015; Lesk et al. 2017). In China, the Qinghai-Tibet Plateau has not been spared from bark beetle infestations, with species such as *Dendroctonus*, *Ips* and *Polygraphus* causing significant damage (Yin et al. 2016; Wang et al. 2021, 2023). There is growing evidence that fungal symbionts play a crucial role in the ability of bark beetles to respond to climate change and cause tree mortality (Netherer et al. 2021). Despite this, the fungal communities associated with some of these beetles remain poorly understood.

Ophiostomatoid fungi, the most well-known fungal partners of bark beetles, belong to the orders Ophiostomatales (Sordariomycetidae, Sordariomycetes, Ascomycota) and Microascales (Hypocreomycetidae, Sordariomycetes, Ascomycota) (De Beer et al. 2013). Amongst these, the Ophiostomatales is the most diverse group associated with bark beetles, with over 300 species reported across 20 genera (De Beer et al. 2022). The genera *Ophiostoma*, *Leptographium* and *Grosmannia* are particularly notable for their species diversity, close symbiotic relationships with insect vectors and inclusion of species that act as virulent pathogens in host trees. *Ophiostoma* is an ancient genus first described by Sydow and Sydow (1919) and its taxonomy has undergone considerable revision since then. Advances in DNA-based taxonomy and the implementation of the "one fungus, one name" nomenclature have clarified the taxonomic status of this genus. Zipfel et al. (2006) demonstrated that *Ceratocystiopsis* and *Grosmannia* are distinct from *Ophiostoma*, based on multi-gene phylogenies of ribosomal DNA and β-tubulin sequences. Subsequently, *Sporothrix*, which was previously considered part of *Ophiostoma*, was recognised as a separate genus, based on four-gene phylogenies and *sporothrix*-like asexual morphs (De Beer et al. 2016). The taxonomic boundaries between *Grosmannia* and *Leptographium* were historically blurred, but new species in the *Grosmannia penicillata* complex were later described under the genus *Grosmannia* (De Beer and Wingfield 2013; Yin et al. 2020). Today, these two genera are clearly distinguished, based on genome-wide sequence data (de Beer et al. 2022). Additionally, *Heinzbutinia*, *Jamesreidia* and *Masuyamyces* have been recognised as distinct from *Ophiostoma*. The current taxonomic framework for ophiostomatalean fungi, which is considered the most authoritative, defines *Ophiostoma*, *Leptographium* and *Grosmannia* as comprising six complexes and four groups, eight complexes and two groups and two complexes and one group, respectively (De Beer et al. 2022).

Many ophiostomatoid fungi have been shown to play a positive role in the success of conifer bark beetles, mainly by producing beetle semio-chemicals, exhausting tree defences, providing nutrition and promoting environmental adaptation (Raffa et al. 2015). *Grosmannia penicillata* and *Leptographium europhioides* were found to synthesise the beetle aggregation pheromone 2-methyl-3-buten-2-ol and similar functions have been demonstrated in a variety of ophiostomatoid fungi, indicating their ability to regulate beetle mass attacks (Zhao et al. 2015; Kandasamy et al. 2019, 2023). In contrast, *Endoconidiophora polonica* can skilfully degrade the phenolic defence compounds of spruce as a carbon source (Wadke et al. 2016), indirectly providing nutrients for its vector,

I. typographus. Fungal associates of *D. ponderosae*, *Leptographium clavigerum*, have been shown to contribute to host mortality by triggering the pine tree myriad defence responses (Fortier et al. 2024). Interestingly, the expression of high-altitude adaption-related genes in *Ips nitidus* was upregulated after feeding on *Ophiostoma bicolor*, suggesting that fungal symbionts may promote the adaptation of insect vectors to extreme environments (Wang et al. 2023).

The genus *Polygraphus* is a secondary pest; however, in recent years, it has been reported to cause an increase in tree mortality in Eurasian coniferous forests (Yin et al. 1984; Viklund et al. 2019). This genus is widely distributed in China and mainly attacks conifers, with a few species using hardwoods as a host (Yin et al. 1984). Only a few fungal associates of *Polygraphus* have been reported, most of which have been isolated from mites associated with beetles. Yin et al. (2016, 2019, 2020) successively reported seven ophiostomatalean species associated with *Polygraphus poligraphus*, three of which were subsequently isolated from beetle mite associates by Chang et al. (2020). In addition, 11 ophiostomatalean species have been isolated from mites associated with *Polygraphus aterrimus*, *P. poligraphus*, *Polygraphus szemaoensis*, *Polygraphus verrucifrons* and *Polygraphus* sp. in Yunnan and Qinghai Provinces (Chang et al. 2017, 2020). Overall, only 18 species from six genera (*Graphilbum*, *Grosmannia*, *Leptographium*, *Masuyamyces*, *Ophiostoma* and *Sporothrix*) associated with five *Polygraphus* beetles were recorded in the two Provinces (Table 1). Although 16 species of this genus have been recorded (Yin et al. 1984; Huang and Lu 2015), most of their fungal associates remain unknown.

Table 1. Ophiostomatalean fungi isolated from *Polygraphus* beetles and their mite associates reported from China.

Fungal species	Host	Beetle vector	Location	Reference[1]
Graphilbum kesiyae	*Pinus kesiya*	*Polygraphus* sp.; *P. aterrimus*; *P. szemaoensis*	Simao and Ning'er, Yunnan, China	Chang et al. (2017)*
Gra. puerense	*P. kesiya*	*P. szemaoensis*	Ning'er Yunnan, China	Chang et al. (2017)*
Grosmannia crassifolia	*Picea crassifolia*	*P. poligraphus*	Zeku, Qinghai, China	Yin et al. (2020)
G. maixiuense	*P. crassifolia*	*P. poligraphus*	Zeku, Qinghai, China	Yin et al. (2020)
G. xianmiense	*P. crassifolia*	*P. poligraphus*	Zeku and Menyuan, Qinghai, China	Yin et al. (2020); Chang et al. (2020)*
Leptographium breviscapum	*P. crassifolia*	*P. poligraphus*	Zeku, Qinghai, China	Yin et al. (2019); Chang et al. (2020)*
L. conjunctum	*P. kesiya*	*Polygraphus* sp.	Ning'er Yunnan, China	Chang et al. (2017)*
L. xiningense	*P. crassifolia*	*P. poligraphus*	Menyuan, Qinghai, China	Yin et al. (2019)
L. yunnanense	*P. kesiya*	*P. szemaoensis*; *Polygraphus* sp.	Ning'er Yunnan, China	Chang et al. (2017)*
Masuyamyces acarorum	*P. kesiya*	*P. szemaoensis*	Ning'er Yunnan, China	Chang et al. (2017)*
Ophiostoma ainoae	*P. crassifolia*	*P. poligraphus*	Zeku, Qinghai, China	Yin et al. (2016); Chang et al. (2020)*
O. bicolor	*P. crassifolia*	*P. poligraphus*	Zeku, Qinghai, China	Chang et al. (2020)*
O. ips	*P. kesiya*	*P. szemaoensis*; *Polygraphus* sp.	Simao and Ning'er, Yunnan, China	Chang et al. (2017)*
O. nitidum	*P. crassifolia*	*P. poligraphus*	Zeku, Qinghai, China	Chang et al. (2020)*
O. qinghaiense	*P. crassifolia*	*P. poligraphus*	Zeku, Qinghai, China	Yin et al. (2016)
O. quercus	*P. kesiya*; *P. yunnanensis*	*P. verrucifrons*; *P. szemaoensis*	Simao and Ning'er, Yunnan, China	Chang et al. (2017)*
O. shangrilae	*P. crassifolia*	*P. poligraphus*	Zeku, Qinghai, China	Chang et al. (2020)*
Sporothrix nebularis	*P. kesiya*	*Polygraphus* sp.	Ning'er Yunnan, China	Chang et al. (2017)*

[1] *represents the references on fungal isolation from mites associated with *Polygraphus* beetles.

In the present study, a survey of fungi associated with *P. poligraphus* and *Polygraphus rudis* was conducted on the Qinghai-Tibet Plateau between 2019 and 2020. We sought to increase our understanding of the fungal assemblages associated with *Polygraphus* beetles, based on the accurate identification and comparison of fungal associates across geographic ranges, hosts and beetle vectors.

Materials and methods

Sample collection and isolation

Adult beetles of *P. poligraphus* and *P. rudis* and/or their galleries were collected during the emergence period from four sites on the north-eastern and southern Qinghai-Tibet Plateau from 2019 to 2020 (Suppl. material 1: table S1). The branches or trunks of the host tree damaged by the beetles were cut into one-metre-long logs and brought back to the laboratory. After peeling the bark, 15 vigorous adults and/or their fresh galleries were selected for fungal isolation from each *Polygraphus* species at each sampling site. Each adult was separated into approximately 15 tissue pieces and transferred to the surface of 2% water agar. The galleries were surface-disinfected with 1.5% sodium hypochlorite and then placed on the surface of 2% water agar. After incubation in the dark at 25 °C, single hyphal tips were transferred to the surface of 2% malt extract agar (MEA) medium to purify the fungal isolates. All strains were deposited in the culture collection at the Forest Pathology Laboratory of the Chinese Academy of Forestry (CXY). Representative strains were deposited at the China Forestry Culture Collection Center, Beijing, China (CFCC).

Morphological studies

The morphological structure of each pure culture was carefully observed using an Olympus BX43 microscope (Olympus Corporation, Tokyo, Japan) and recorded using a BioHD-A20c colour digital camera (FluoCa Scientific, China, Shanghai). For the holotype of the new species, we measured the lengths and widths of 30 reproductive structures and presented the following format: (minimum–) mean minus standard deviation–mean plus standard deviation (–maximum). 5-mm diameter agar plugs were transferred from the actively growing margin of fungal colonies and placed in the centre of a 90-mm-diameter Petri plate containing 2% MEA to conduct cultural character studies. Five replicates of culture were incubated at temperatures ranging from 5 °C to 40 °C at 5 °C intervals in darkness. The colony diameters were measured daily until the mycelia reached the margins of the Petri dishes. Culture features were observed and recorded daily until the colonies no longer showed any significant changes. All the data from the type specimens were deposited in MycoBank (www.MycoBank.org).

DNA extraction, PCR amplification and sequencing

Actively growing mycelia of each representative strain were collected for DNA extraction using an Invisorb Spin Plant Mini Kit (Tiangen, Beijing, China), following the manufacturer's instructions. The internal transcribed spacer regions 1 and 2 of the nuclear ribosomal DNA operon, including the 5.8S region (ITS), internal transcribed spacer 2, part of the 28S of the rDNA operon (ITS2-LSU), β-tubulin gene

region (*tub2*) and transcription elongation factor 1-α gene region (*tef1-α*) were amplified using the primer pairs of ITS1-F/ITS4 (White et al. 1990; Gardes and Bruns 1993), ITS3/LR3 (Vilgalys and Hester 1990; White et al. 1990), Bt2a/Bt2b (Glass and Donaldson 1995) or T10/Bt2b (O'Donnell and Cigelnik 1997) or EF1F/EF2R (Jacobs et al. 2004), respectively, using 2 × Taq PCR MasterMix (Tiangen, Beijing, China), following the manufacturer's instructions. PCR and sequencing were performed according to protocols described by Wang et al. (2020, 2021).

Phylogenetic analysis

Newly-obtained sequences were identified using a standard nucleotide BLAST search in NCBI and deposited in GenBank. Reference sequences in the phylogenetic analyses were confirmed, based on the BLAST results, relevant literature and sequences downloaded from GenBank. MAFFT v.7 (Katoh et al. 2019) was used to construct the multiple sequence alignment. Molecular Evolutionary Genetic Analyses (MEGA) 7.0 (Kumar et al. 2016) were used to edit and/or splice alignments to generate combined gene datasets.

Maximum Likelihood (ML) analyses were conducted using RAxML-HPC v.8.2.3 (Stamatakis 2014) with 1000 replicates using the GTRGAMMA model. The bootstrap support values of the nodes were estimated using 1,000 bootstrap replicates after retaining the best tree. jModelTest v.2.1.7 (Darriba et al. 2012) was used to determine the best substitution models for conducting Bayesian Inference (BI) analyses in MrBayes v. 3.1.2 (Ronquist and Huelsenbeck 2003). Four Markov Chain Monte Carlo (MCMC) chains were run simultaneously from a random starting tree for 10,000,000 generations. The trees were sampled every 100 generations. Posterior probabilities were calculated, based on the remaining trees after discarding the first 25% of the sampled trees. Phylogenetic trees were edited and polished using FigTree v.1.4.3 (http://tree.bio.ed.ac.uk/software/figtree/) and Adobe Illustrator CS6. The final sequence datasets were submitted to TreeBASE (31618).

Results

Sampling collection and fungal isolation

In the present study, 442 ophiostomatalean strains were isolated from 75 vigorous adult *Polygraphus* species and 180 fresh galleries of *Picea crassifolia* and *Pinus griffithii*. Morphological characterisations and *tub2* or ITS sequence features, based on standard nucleotide BLAST searches at GenBank, were used for preliminary identification. Subsequently, 49 representative strains were selected for detailed morphological and phylogenetic analyses (Table 2).

Phylogenetic analysis

Grosmannia spp. and *Leptographium* spp.

The ITS2-LSU dataset was used to construct phylogenetic inferences for the two genera. The dataset contained 610 characters, including gaps and the best evolutionary model for BI analysis was estimated to be GTR+I+G.

Table 2. Representative strains of ophiostomatalean fungi isolated from *Polygraphus* bark beetles in this study. [1] CFCC: the China Forestry Culture Collection Center; CXY: the culture collection at the Forest Pathology Laboratory of the Chinese Academy of Forestry.

Species	Taxon	Isolate no[1]	Host	Insect vector	Location	GenBank accession no		
						ITS or ITS2-LSU	tub2	tef1-α
Grosmannia								
G. penicillata complex								
G. crassifolia	1	CFCC57904	*Picea crassifolia*	*Polygraphus poligraphus*	Zeku, Qinghai, China	PQ166546	PQ166449	PQ166498
G. maixiuensis	2	CFCC57902	*P. crassifolia*	*P. poligraphus*	Zeku, Qinghai, China	PQ166547	PQ166450	PQ166499
		CFCC57903	*P. crassifolia*	*P. poligraphus*	Zeku, Qinghai, China	-	PQ166451	PQ166500
Grosmannia sp. 1	3	CFCC57905	*P. crassifolia*	*P. rudis*	Zeku, Qinghai, China	PQ166548	PQ166452	PQ166501
		CFCC57906	*P. crassifolia*	*P. rudis*	Zeku, Qinghai, China	-	PQ166453	PQ166502
		CFCC57907	*P. crassifolia*	*P. poligraphus*	Qilian, Qinghai, China	-	PQ166454	PQ166503
		CFCC57908	*P. crassifolia*	*P. poligraphus*	Qilian, Qinghai, China	-	PQ166455	PQ166504
Leptographium								
L. lundbergii complex								
L. griffithii	4	CFCC57893	*Pinus griffithii*	*P. rudis*	Yadong, Tibet, China	PQ166549	PQ166456	PQ166505
		CFCC57894	*P. griffithii*	*P. rudis*	Yadong, Tibet, China	-	PQ166457	PQ166506
		CFCC57895	*P. griffithii*	*P. rudis*	Yadong, Tibet, China	-	PQ166458	PQ166507
L. jilongense	5	CFCC57896	*P. griffithii*	*P. rudis*	Jilong, Tibet, China	PQ166550	PQ166459	PQ166508
L. pseudojilongense	6	CFCC57901	*P. griffithii*	*P. rudis*	Jilong, Tibet, China	PQ166551	PQ166460	PQ166509
		CXY3348	*P. griffithii*	*P. rudis*	Jilong, Tibet, China	-	PQ166461	PQ166510
		CXY3349	*P. griffithii*	*P. rudis*	Jilong, Tibet, China	-	PQ166462	PQ166511
L. yadongense	7	CFCC57897	*P. griffithii*	*P. rudis*	Yadong, Tibet, China	PQ166552	PQ166463	PQ166512
		CFCC57898	*P. griffithii*	*P. rudis*	Yadong, Tibet, China	-	PQ166464	PQ166513
		CFCC57899	*P. griffithii*	*P. rudis*	Yadong, Tibet, China	-	PQ166465	PQ166514
		CFCC57900	*P. griffithii*	*P. rudis*	Yadong, Tibet, China	-	PQ166466	PQ166515
L. olivaceum complex								
L. breviscapum	8	CFCC57890	*P. crassifolia*	*P. poligraphus*	Zeku, Qinghai, China	PQ166553	PQ166467	PQ166516
		CFCC57891	*P. crassifolia*	*P. poligraphus*	Zeku, Qinghai, China	-	PQ166468	PQ166517
		CFCC57892	*P. crassifolia*	*P. poligraphus*	Zeku, Qinghai, China	-	PQ166469	PQ166518
Ophiostoma								
O. clavatum complex								
O. pseudobrevipilosi	9	CFCC57916	*P. griffithii*	*P. rudis*	Yadong, Tibet, China	-	PQ166470	-
		CFCC57917	*P. griffithii*	*P. rudis*	Yadong, Tibet, China	PQ166530	PQ166471	-
		CFCC57918	*P. griffithii*	*P. rudis*	Yadong, Tibet, China	-	PQ166472	-
		CFCC57919	*P. griffithii*	*P. rudis*	Yadong, Tibet, China	-	PQ166473	-
O. stebbingi	10	CFCC57920	*P. griffithii*	*P. rudis*	Jilong, Tibet, China	-	PQ166474	PQ166519
		CFCC57921	*P. griffithii*	*P. rudis*	Jilong, Tibet, China	PQ166531	PQ166475	-
		CFCC57922	*P. griffithii*	*P. rudis*	Jilong, Tibet, China	-	PQ166476	-
Ophiostoma sp. 1	11	CFCC57923	*P. griffithii*	*P. rudis*	Jilong, Tibet, China	PQ166532	PQ166477	PQ166520
		CFCC57924	*P. griffithii*	*P. rudis*	Jilong, Tibet, China	-	PQ166478	-
		CFCC57925	*P. griffithii*	*P. rudis*	Jilong, Tibet, China	-	PQ166479	-
O. ips complex								
O. bicolor	12	CFCC57909	*P. crassifolia*	*P. poligraphus*	Zeku, Qinghai, China	PQ166533	PQ166480	-
		CFCC57910	*P. crassifolia*	*P. poligraphus*	Zeku, Qinghai, China	-	PQ166481	-
		CFCC57911	*P. crassifolia*	*P. poligraphus*	Zeku, Qinghai, China	-	PQ166482	-
		CFCC57912	*P. crassifolia*	*P. poligraphus*	Qilian, Qinghai, China	-	PQ166483	-
O. shigatsense	13	CFCC57913	*P. griffithii*	*P. rudis*	Jilong, Tibet, China	PQ166534	PQ166484	-
		CFCC57914	*P. griffithii*	*P. rudis*	Jilong, Tibet, China	-	PQ166485	-
		CFCC57915	*P. griffithii*	*P. rudis*	Jilong, Tibet, China	-	PQ166486	-

Species	Taxon	Isolate no[1]	Host	Insect vector	Location	GenBank accession no		
						ITS or ITS2-LSU	tub2	tef1-α
Group A								
O. maixiuense	14	CFCC57930	*P. griffithii*	*P. rudis*	Jilong, Tibet, China	PQ166535	PQ166487	-
		CFCC57931	*P. griffithii*	*P. rudis*	Jilong, Tibet, China	PQ166536	PQ166488	-
		CFCC57932	*P. crassifolia*	*P. poligraphus*	Zeku, Qinghai, China	PQ166537	PQ166489	-
		CFCC57933	*P. crassifolia*	*P. poligraphus*	Zeku, Qinghai, China	PQ166538	PQ166490	-
		CFCC57934	*P. griffithii*	*P. rudis*	Yadong, Tibet, China	PQ166539	PQ166491	-
		CFCC57935	*P. griffithii*	*P. rudis*	Yadong, Tibet, China	PQ166540	PQ166492	-
O. pacis	15	CFCC57936	*P. crassifolia*	*P. poligraphus*	Zeku, Qinghai, China	PQ166541	PQ166493	-
O. sanum	16	CFCC57926	*P. crassifolia*	*P. rudis*	Zeku, Qinghai, China	PQ166542	PQ166494	-
		CFCC57927	*P. crassifolia*	*P. rudis*	Zeku, Qinghai, China	PQ166543	PQ166495	-
		CFCC57928	*P. crassifolia*	*P. rudis*	Zeku, Qinghai, China	PQ166544	PQ166496	-
		CFCC57929	*P. crassifolia*	*P. rudis*	Zeku, Qinghai, China	PQ166545	PQ166497	-

The results showed that our eight representative isolates nested into three complexes, namely the *G. penicillata*, *L. lundbergii* and *L. olivaceum* complexes (Fig. 1). Amongst these, the *G. penicillata* complex belongs to *Grosmannia*, whereas the *L. lundbergii* and *L. olivaceum* complexes belong to *Leptographium*. Subsequently, we constructed the phylogenetic inference of *tub2*, *tef1-α* and the concatenated (*tub2*+*tef1-α*) datasets for each complex.

Grosmannia penicillata complex

The *tub2*, *tef1-α* and concatenated (*tub2*+*tef1-α*) datasets were aligned (containing 402, 694 and 1096 characters, including gaps, respectively) and used to construct the phylogenetic inference. The best models of the three datasets for BI analysis were estimated as HKY+I (*tub2* dataset) and GTR+G (*tef1-α* and concatenated datasets). Based on the concatenated tree (Fig. 2), the seven isolates formed three separate well-supported terminal clades, representing two known and one undescribed taxa: *G. crassifolia* (Taxon 1), *G. maixiuensis* (Taxon 2) and *Grosmannia* sp. 1 (Taxon 3). These three species formed a subclade with *G. chlamydata* and *G. nitidi* that was phylogenically consistent, based on the three datasets (Fig. 2, Suppl. material 2: figs S1, S2).

Leptographium lundbergii complex

The *tub2*, *tef1-α* and concatenated (*tub2*+*tef1-α*) datasets were aligned (containing 373, 666 and 1039 characters, including gaps, respectively) and used to construct the phylogenetic inference. The best models of the three datasets for BI analysis were SYM+I, HKY+G and GTR+G. Based on the concatenated tree (Fig. 3), our ten isolates formed four separate well-supported terminal clades, representing three known (Taxon 4: *L. griffithii*; Taxon 5: *L. jilongense*; Taxon 7: *L. yadongense*) and one undescribed (Taxon 6) taxa. Taxa 4, 5 and 6 were sister species and formed a subclade with *L. panxianense*, *L. yunnanensis*, *L. puerense*, *L. wushanense* and *L. conjunctum*, all of which were isolated from *Pinus* trees in southwest China (Fig. 3, Suppl. material 2: figs S3, S4). The four isolated strains were identical in sequence to the two strains isolated from *Ips schmutzenhoferi*, representing *L. yadongense*, which was a phylogenetic sister to *L. sejilanum* (Fig. 3, Suppl. material 2: figs S3, S4).

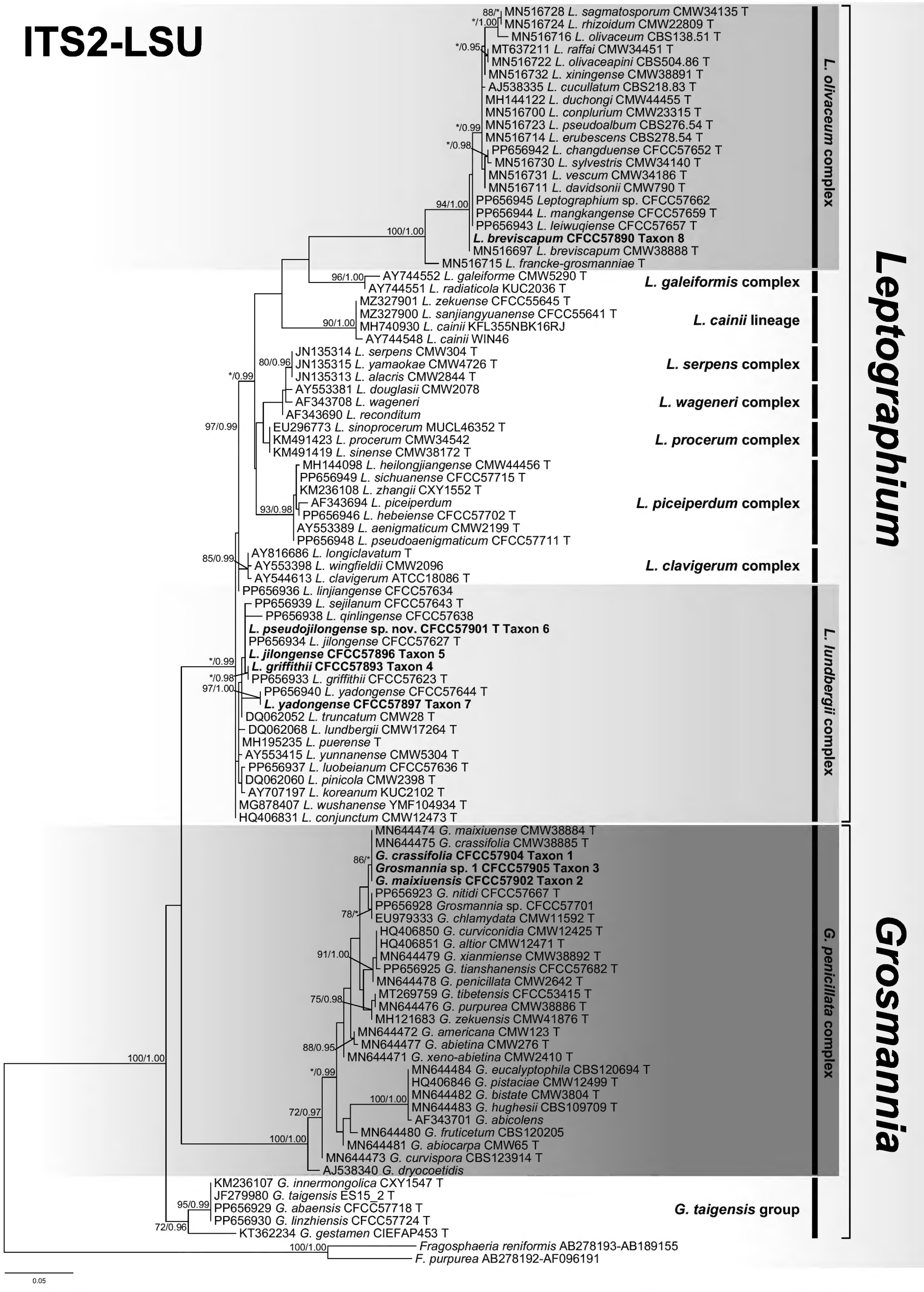

Figure 1. Phylogram of *Grosmannia* spp. and *Leptographium* spp. based on ITS2-LSU sequence data. The ML bootstrap support values ≥ 70% and posterior probability values ≥ 0.9 are recorded at the nodes. T = ex-type isolates.

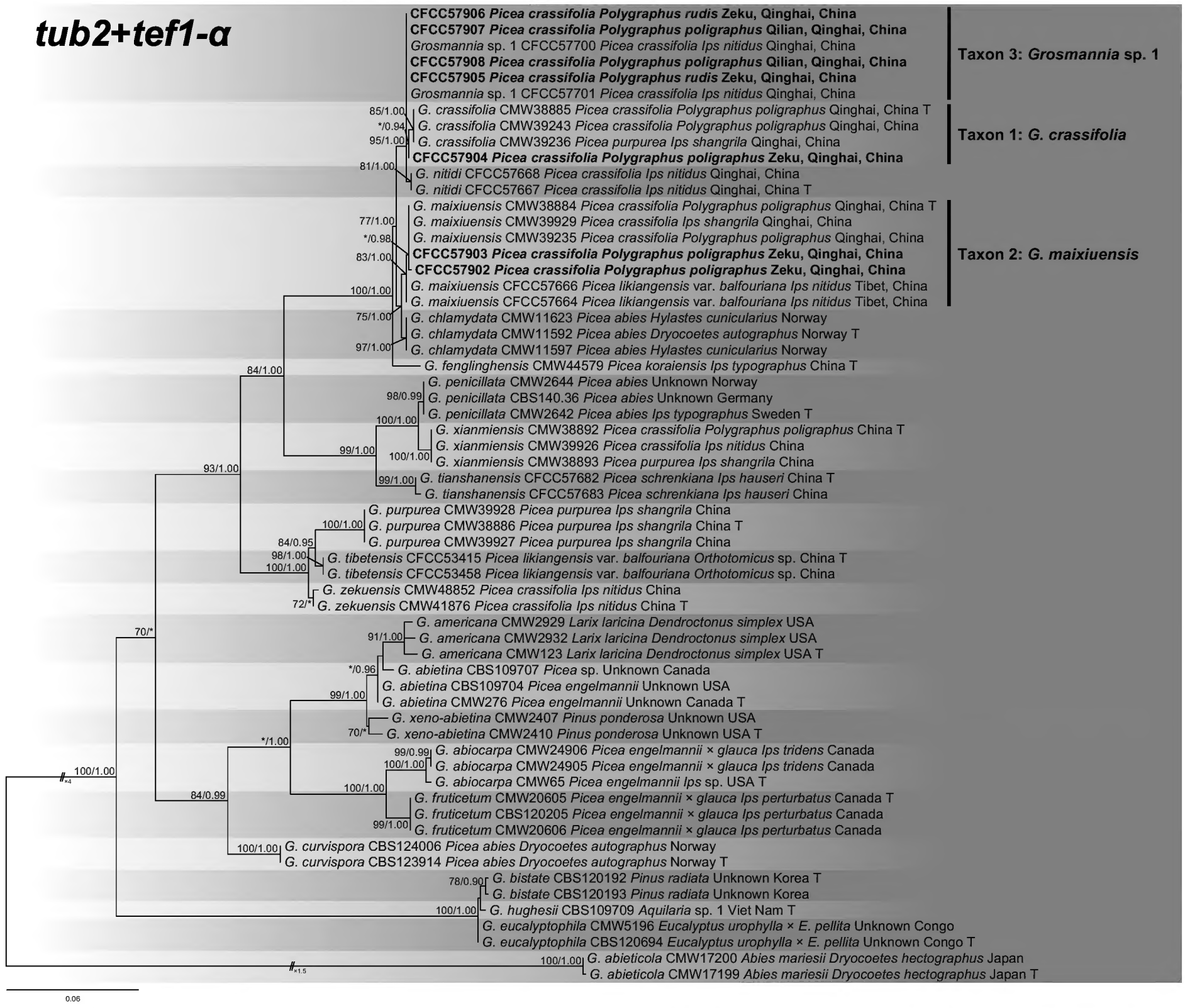

Figure 2. Phylogram of *Grosmannia penicillata* complex (including Taxa 1–3) based on combined (*tub2*+*tef1-α*) sequence data. The ML bootstrap support values ≥ 70% and posterior probability values ≥ 0.9 are recorded at the nodes. T = ex-type isolates.

Leptographium olivaceum complex

The *tub2*, *tef1-α* and concatenated (*tub2*+*tef1-α*) datasets were aligned (containing 278, 677 and 955 characters, including gaps, respectively) and used to construct the phylogenetic inference. The best models of the three datasets for BI analysis were estimated as (*tub2* dataset) and GTR+G (*tef1-α* and concatenated datasets). Based on the concatenated tree (Fig. 4), the three isolates formed a separate, well-supported, terminal clade representing *L. breviscapum* (Taxon 8). The 10 strains of *L. breviscapum* formed a subclade with *L. leiwuqiense*, *L. mangkangense* and *Leptographium* sp. 1, all of which were isolated from *Picea* trees on the Qinghai-Tibet Plateau (Fig. 4, Suppl. material 2: figs S5, S6).

Ophiostoma spp.

An ITS dataset was used to construct a phylogenetic inference for this genus. The dataset contained 743 characters, including gaps and the best evolutionary model for BI analysis was estimated to be GTR+I+G. The results showed

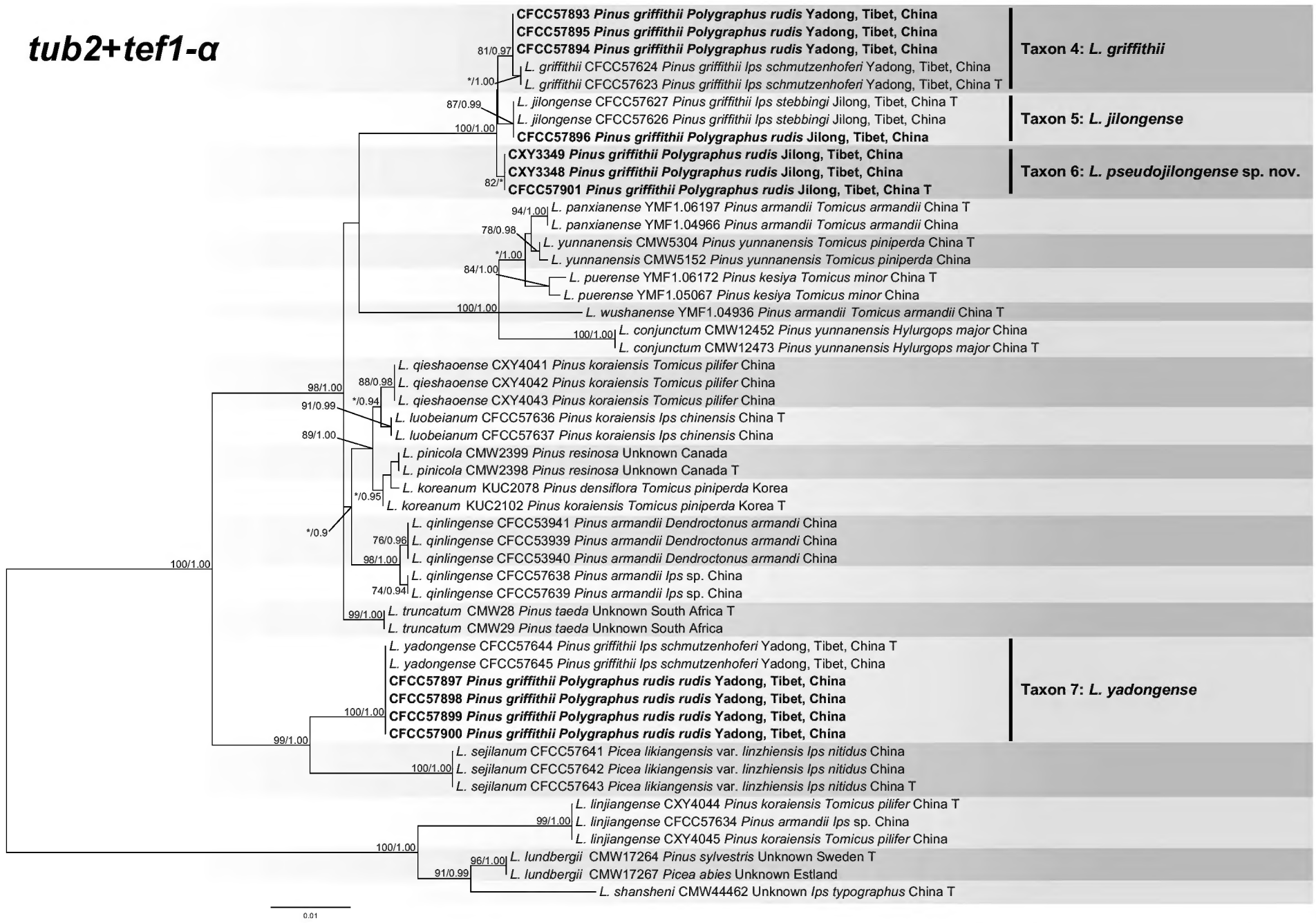

Figure 3. Phylogram of *Leptographium lundbergii* complex (including Taxa 4–7) based on combined (*tub2+tef1-α*) sequence data. The ML bootstrap support values ≥ 70% and posterior probability values ≥ 0.9 are recorded at the nodes. T = ex-type isolates.

that our eight representative isolates nested into two complexes and one Group A, namely the *O. clavatum* complex, *O. ips* complex and Group A (Fig. 5). Subsequently, we constructed the phylogenetic inference of *tub2*, *tef1-α* and/or the concatenated (*tub2+tef1-α* or ITS+*tub2*) datasets for each complex or Group.

Ophiostoma clavatum complex

The *tub2*, *tef1-α* and concatenated (*tub2+tef1-α*) datasets were aligned (containing 438, 594 and 1032 characters, including gaps, respectively) and used to construct the phylogenetic inference. The best models of the three datasets for BI analysis were estimated as HKY+I, GTR+G and GTR+I+G. Based on the concatenated tree (Fig. 6), our ten isolates formed three separate well-supported terminal clades, representing two known (Taxon 9: *O. pseudobrevipilosi*; Taxon 10: *O. stebbingi*) and one undescribed (Taxon 11: *Ophiostoma* sp. 1) taxa. *Ophiostoma pseudobrevipilosi*, *O. stebbingi* and *Ophiostoma* sp. 1 formed the main subclade in this complex with *O. ainoae*, *O. brevipilosi*, *O. pseudobrevipilosi*, *O. schmutzenhoferi*, *O. shangrilae* and *O. yadongense* (Fig. 6, Suppl. material 2: figs S7, S8).

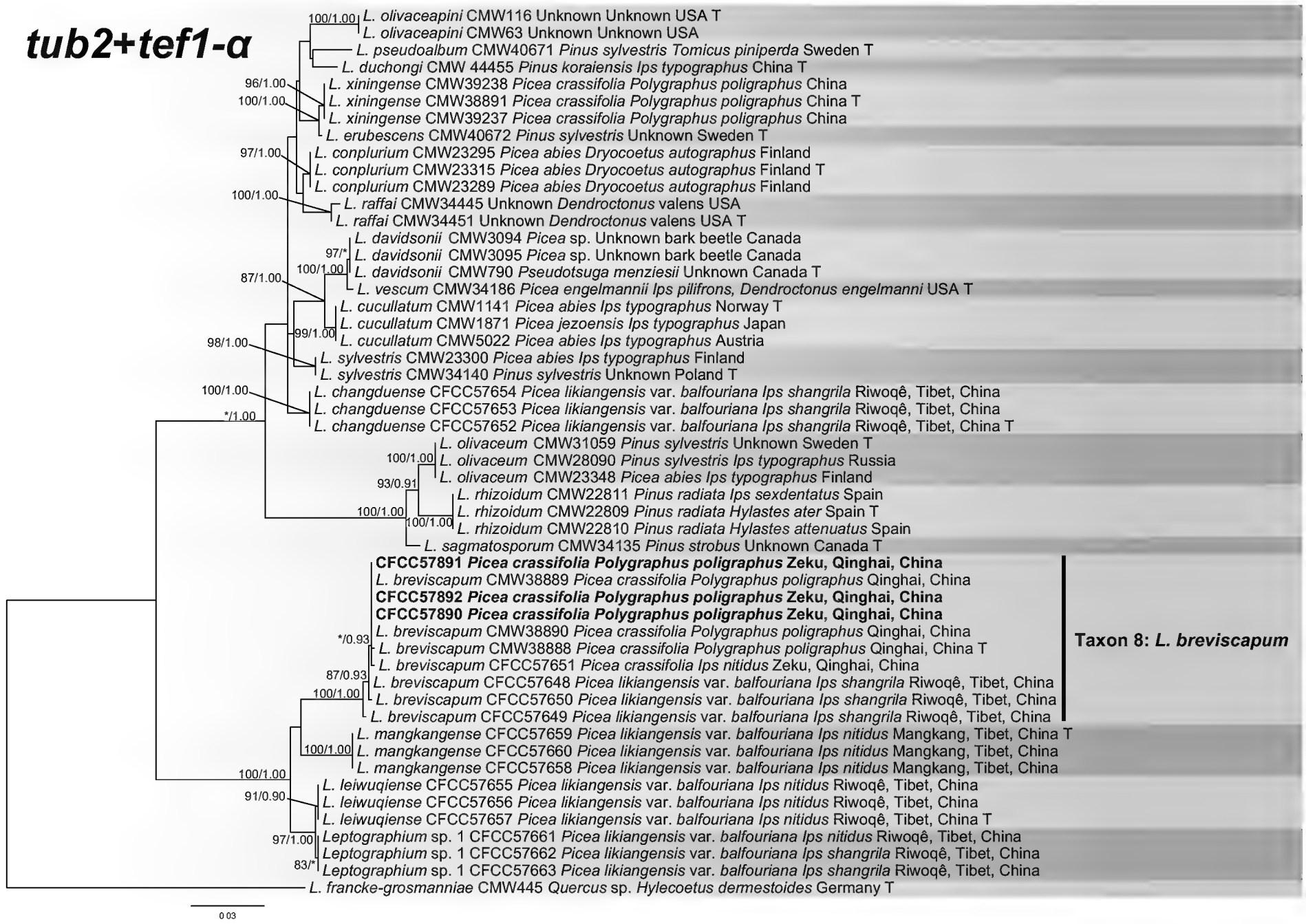

Figure 4. Phylogram of *Leptographium olivaceum* complex (including Taxon 8) based on combined (*tub2*+*tef1-α*) sequence data. The ML bootstrap support values ≥ 70% and posterior probability values ≥ 0.9 are recorded at the nodes. T = ex-type isolates.

Ophiostoma ips complex

The *tub2* dataset was aligned (containing 274 characters including gaps) and used to construct a phylogenetic inference. The best model of the three datasets for BI analysis was estimated to be HKY+I. The seven isolates formed two clades: *O. bicolor* (Taxon12) and *O. shigatsense* (Taxon 13) (Fig. 7).

Group A

The ITS, *tub2* and concatenated (ITS+*tub2*) datasets were aligned (containing 685, 445 and 1130 characters, including gaps) and used to construct the phylogenetic inference. The best models of the three datasets for BI analysis were estimated to be GTR+I+G (ITS dataset) and GTR+G (ITS and concatenated datasets). Based on the concatenated tree (Fig. 8), the 11 isolates formed three separate well-supported terminal clades representing three known taxa (Taxon 14: *O. maixiuense*, Taxon 15: *O. pacis* and Taxon 16: *O. sanum*). *Ophiostoma maixiuense* and *O. sanum* showed intraspecific sequence variation and were phylogenetic sisters to *O. aggregatum* and *O. pacis* (Fig. 8, Suppl. material 2: figs S9, S10).

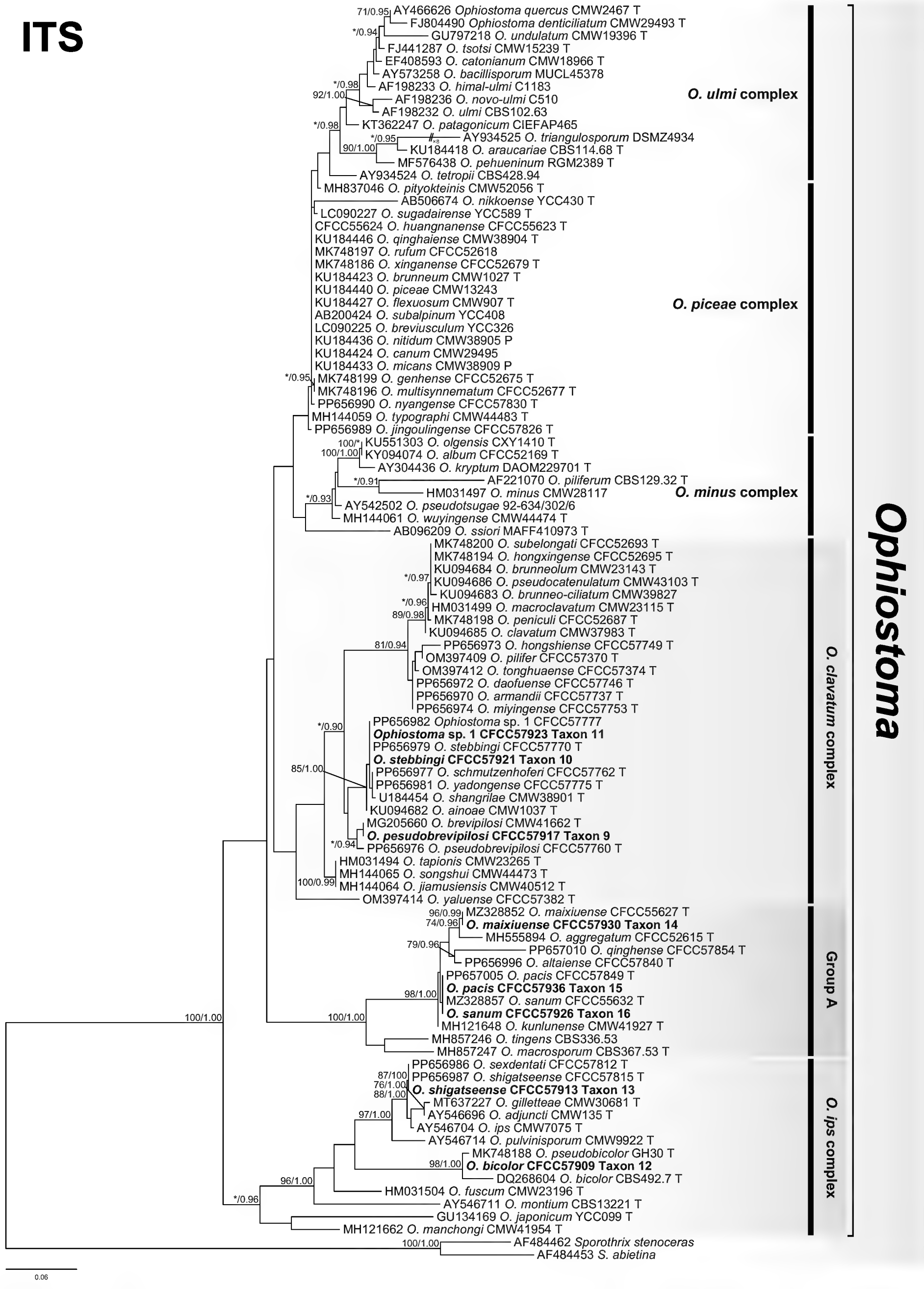

Figure 5. Phylogram of *Ophiostoma* spp. based on ITS sequence data. The ML bootstrap support values ≥ 70% and posterior probability values ≥ 0.9 are recorded at the nodes. T = ex-type isolates.

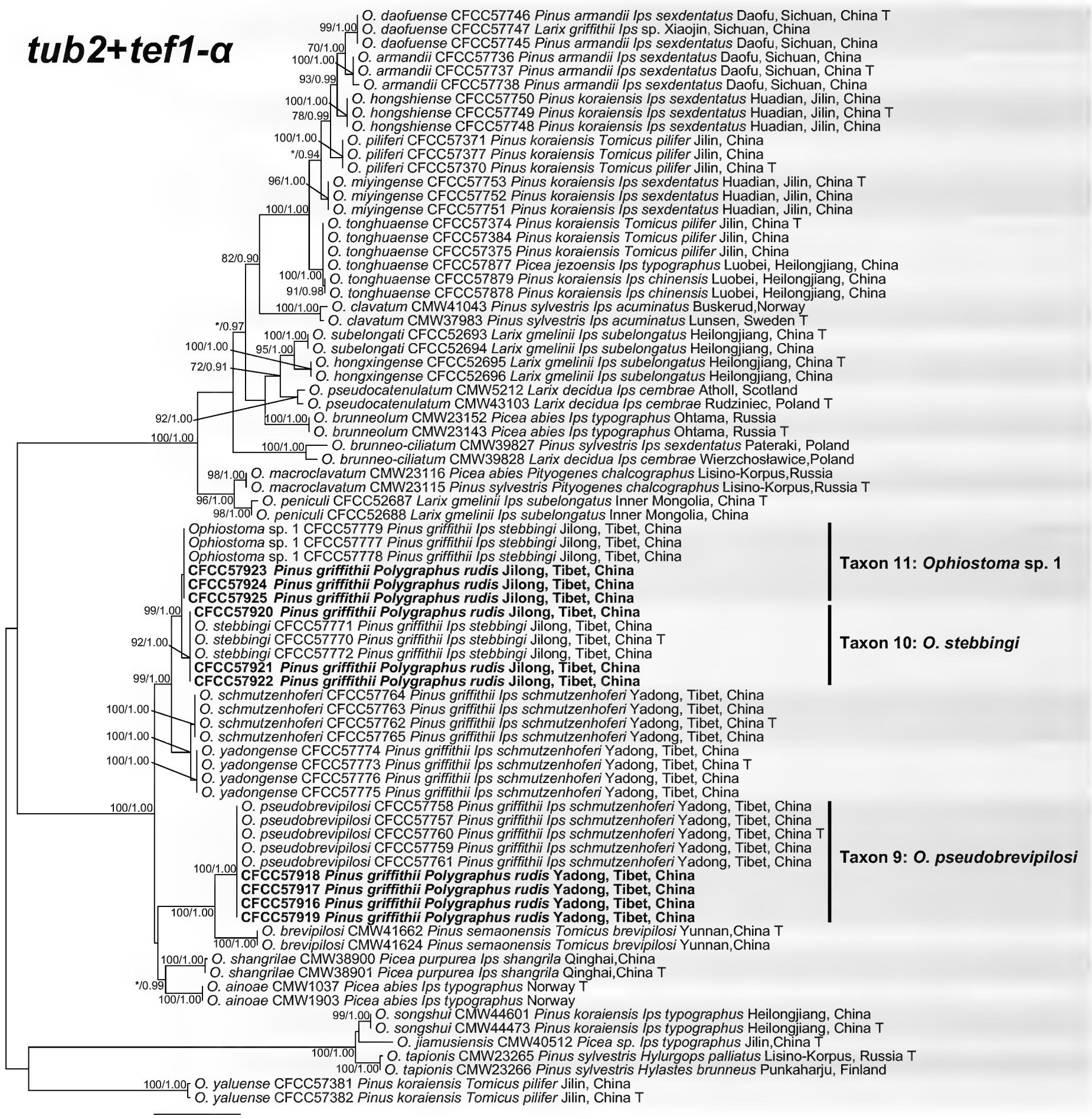

Figure 6. Phylogram of *Ophiostoma clavatum* complex (including Taxa 9–11) based on combined (*tub2+tef1-α*) sequence data. The ML bootstrap support values ≥ 70% and posterior probability values ≥ 0.9 are recorded at the nodes. T = ex-type isolates.

Taxonomy

***Leptographium pseudojilongense* Z. Wang & Q. Lu, sp. nov.**

MycoBank No: 855413

Taxon 6, Fig. 9

Etymology. The epithet *pseudojilongense* (Latin) refers to its sister species *L. jilongense*.

Holotype. CXY3312.

Description. Sexual morph: not observed. **Asexual morph:** ***Leptographium***-like. ***Conidiophores*** occurring singly, upright, arising directly from the mycelium,

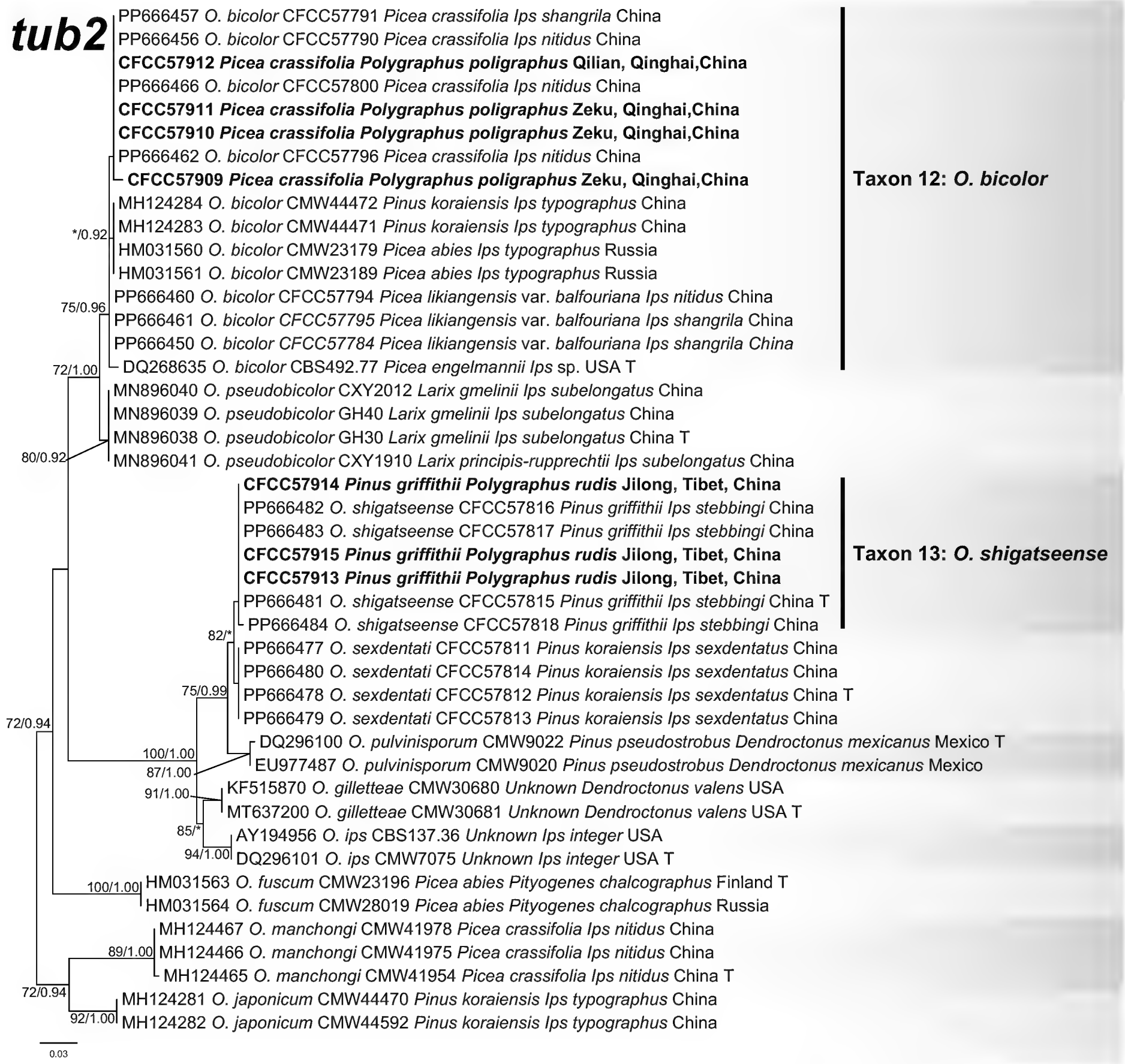

Figure 7. Phylogram of *Ophiostoma ips* complex (including Taxa 12–13) based on *tub2* sequence data. The ML bootstrap support values ≥ 70% and posterior probability values ≥ 0.9 are recorded at the nodes. T = ex-type isolates.

macronematous, mononematous, (247.7–)343.3–484.6(–513.7) µm in length including the conidiogenous apparatus, rhizoid-like structures absent. ***Stipes*** light olivaceous, not constricted, cylindrical, simple, 3–10-septate, (98.8–)103.0–230.0(–301.2) µm in length, (9.0–)11.1–16.9(–18.6) µm wide at base, the basal cell swollen or not, (7.1–)8.5–14.2(–16.6) µm wide below primary branches, apical cell not swollen. ***Conidiogenous apparatus*** (100.8–)180.1–362.1(–417.4) µm in length, excluding the conidial mass, consisting of 1–4 series of branches, the primary branching type B. ***Primary branches*** light olivaceous, cylindrical, (15.4–)19.6–31.8(–35.4) × (6.2–)7.3–10.6(–12.3) µm; ***secondary branches*** light olivaceous, aseptate, (12.4–)13.3–16.7(–18.4) × (6.0–)6.4–9.5(–10.2) µm; ***tertiary branches*** light olivaceous or hyaline, aseptate, (8.0–)8.4–14.0(–16.1) × 5.3–7.6(–8.9) µm. ***Conidiogenous cells*** discrete, 2–3 per branch, smooth or rough, cylindrical, (16.9–)22.2–35.4(–52.6) × (3.9–)4.0–4.8(–5.1) µm. ***Conidia*** hyaline, smooth, aseptate, obovoid, (11.9–)12.9–15.7(–17.9) × (5.5–)6.3–7.8(–8.2) µm.

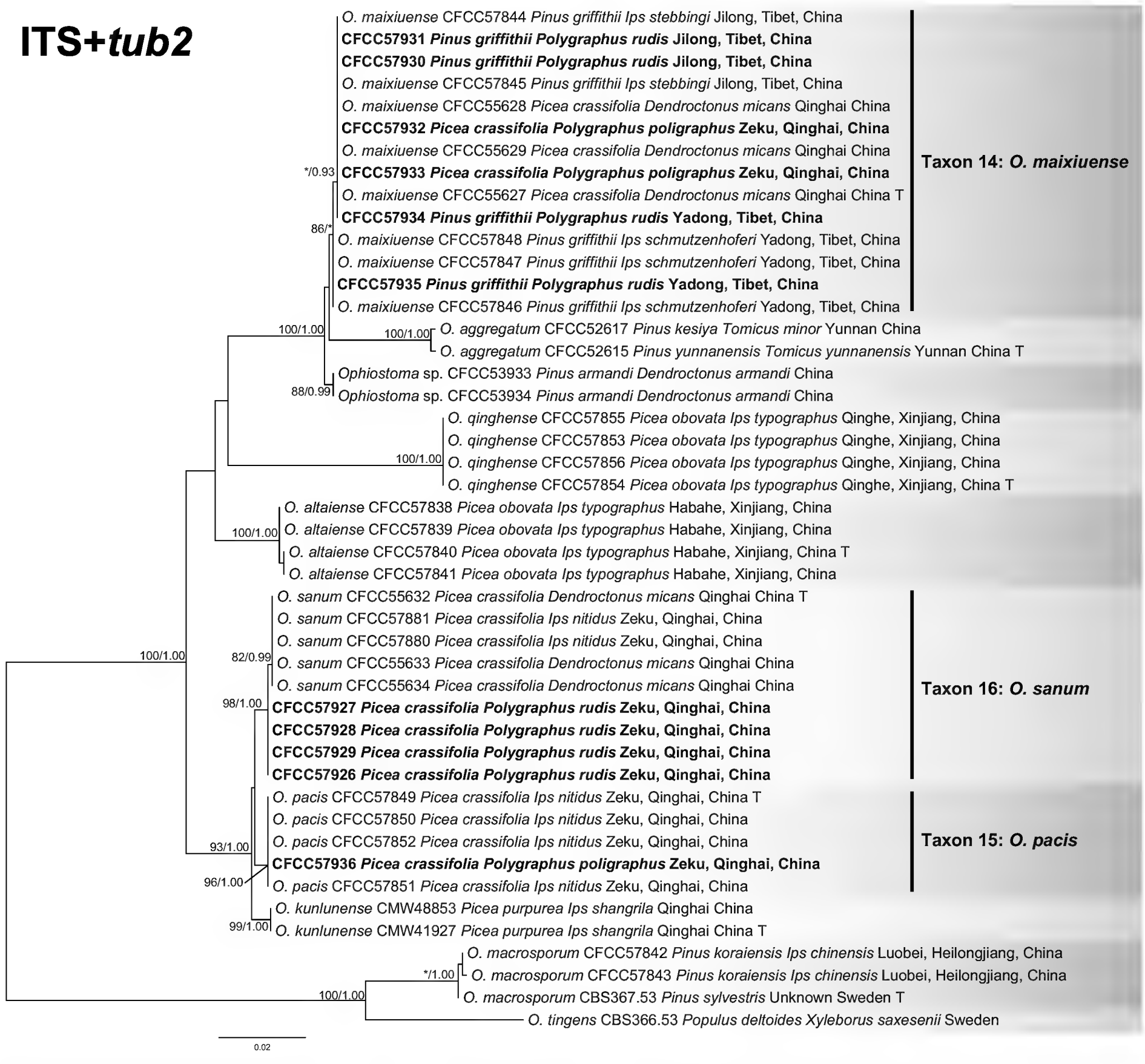

Figure 8. Phylogram of Group A (including Taxa 14–16) based on combined (ITS+*tub2*) sequence data. The ML bootstrap support values ≥ 70% and posterior probability values ≥ 0.9 are recorded at the nodes. T = ex-type isolates.

Culture characters. Colonies on 2% MEA at 25 °C reaching a diameter of 50.1 mm in 4 days, initially hyaline or light white, later becoming light olivaceous from the centre of the colony to the sides, then becoming dark olivaceous, mycelium submerged and superficial with abundant aerial mycelia and the colony margin thinning radially. Optimal temperature for growth was 25 °C, with slow growth observed at 5 °C (45.3 mm in 30 days) and no growth at 35 °C.

Associated insects. *Polygraphus rudis*.

Hosts. *Pinus griffithii*.

Material examined. CHINA • Xizang Autonomous Region, Shigatse City, Jilong County, from *Polygraphus rudis* infesting *Pinus griffithii*, July 2019, Z. Wang and Q. Lu, holotype: CXY3312, ex-type culture CFCC57901, ibid. CXY3348, CXY3349.

Notes. *Leptographium pseudojilongense* was a phylogenetic sister to *L. griffithii* and *L. jilongense* (Fig. 9), both of which were associated with *Pinus griffithii* in Shigatse, Xizang (Wang et al. 2024). *Leptographium pseudojilongense* can be distinguished from *L. griffithii* in the concatenated alignment by 1/373 bp in *tub2*

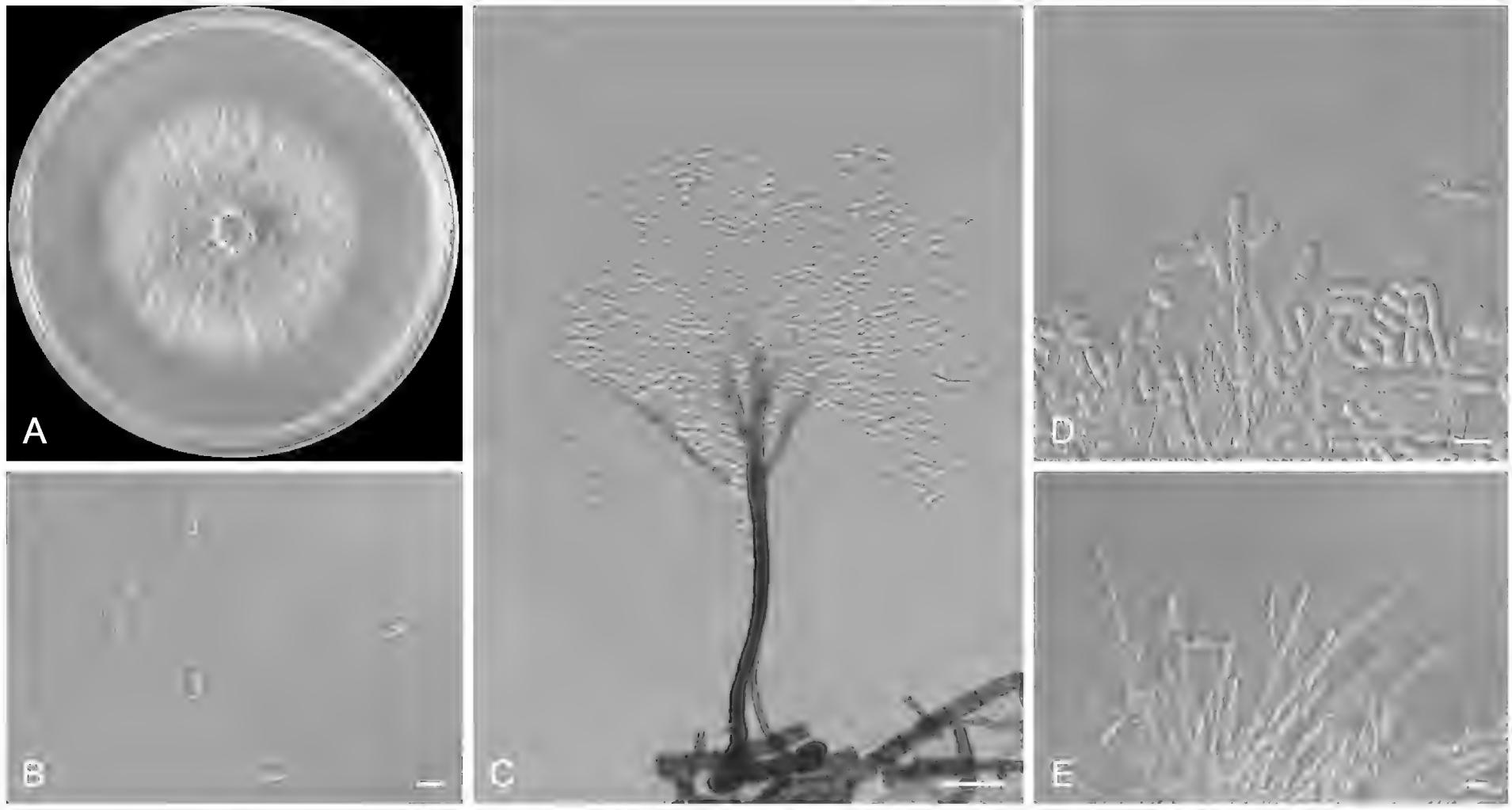

Figure 9. Morphological characteristics of *Leptographium pseudojilongense* sp. nov. (Taxon 9, CXY3312, holotype) **A** four-day-old cultures on 2% MEA **B–E** *Leptographium*-like asexual morph: conidiogenous cells and conidia. Scale bars: 10 µm (**B, D, E**); 40 µm (**C**).

and 3/666 bp in *tef1-α* and from *L. jilongense* in the concatenated alignment by 3/666 bp in *tef1-α*. In terms of morphological characteristics, *L. pseudojilongense* can be distinguished from the other two species by the presence of a *leptographium*-like asexual state, which is absent in the latter two. For culture characteristics, the optimum growth temperature for both was 25 °C, but the former grew slower than the latter two (4 days: 50.1 mm vs. 64.5 and 76.0 mm). At 5 °C, *L. pseudojilongense* was observed growing slowly with 45.3 mm in 30 days, whereas the other two did not grow. Furthermore, *L. pseudojilongense* was isolated from Jilong County, whereas *L. griffithii* and *L. jilongense* were isolated from *Ips schmutzenhoferi* from Yadong County and *Ips stebbingi* from Jilong County, respectively.

Discussion

In total, 442 ophiostomatalean strains representing 16 species were obtained from adult *Polygraphus* beetles and their galleries in *Picea crassifolia* and *Pinus griffithii* on the north-eastern and southern Qinghai-Tibet Plateau. These species were assigned to *Grosmannia* (*G. crassifolia*, *G. maixiuensis* and *Grosmannia* sp. 1 in *G. penicillata* complex), *Leptographium* (*L. griffithii*, *L. jilongense*, *L. pseudojilongense* and *L. yadongense* in *L. lundbergii* complex; *L. breviscapum* in *L. olivaceum* complex) and *Ophiostoma* (*O. pseudobrevipilosi*, *O. stebbingi* and *Ophiostoma* sp. 1 in *O. clavatum* complex; *O. bicolor* and *O. shigatsense* in *O. ips* complex; *O. maixiuense*, *O. pacis* and *O. sanum* in Group A). Amongst them, 12 species were first recorded as associated with *Polygraphus* beetles in China. Yin et al. (2016, 2019, 2020) reported seven ophiostomatalean associates of *P. poligraphus*, but we only collected three of them, which may be because of sample size and sampling time or because the remaining four species are occasional (the previous reports did not count the proportions of each species). To date, three genera (20 species) of

ophiostomatalean fungi have been reported to be associated with *Polygraphus* beetles in China (Yin et al. 2016, 2019, 2020), increasing to six genera (30 species) when the fungi isolated from mites associated with these beetles are included (Chang et al. 2017, 2020), showing an abundance of species diversity (Tables 1, 3).

The dominant species in this study were *O. maixiuense*, *O. bicolor*, *L. yadongense* and *O. pseudobrevipilosi*, representing 20.8%, 18.1%, 17.4% and 13.4% of the ophiostomatalean isolates, respectively, while the other 12 species all had < 10% (Table 3). *Ophiostoma maixiuense* was first reported to be associated with *Dendroctonus micans* infesting *P. crassifolia* on the north-eastern Qinghai-Tibet Plateau (Wang et al. 2021). This species was also obtained from *P. poligraphus* from the same host tree and sampling location. In addition, although several fungal associates of *P. rudis*, *I. schmutzenhoferi* and *I. stebbingi* have been isolated from *P. griffithii* in the Jilong and Yadong Counties on the southern Qinghai-Tibet Plateau, only *O. maixiuense* was shared (Table 3; Wang et al. (2024)). Therefore, this species may be widespread on the Qinghai-Tibet Plateau and its pathogenicity to host trees and association with bark beetles deserve further study. *Ophiostoma bicolor* is frequently associated with bark beetles that harm spruce trees, such as some *Ips* and *Polygraphus* beetles in the Northern Hemisphere (Yamaoka et al. 1997; Kirisits 2004; Alamouti et al. 2007; Chang et al. 2019, 2020; Wang et al. 2021, 2024). It plays multiple roles in the association between beetles and spruce. Solheim (1988) found that it is weakly pathogenic to spruce trees, which may induce the host defence rather than deplete it (Liu et al. 2022). This is not necessarily beneficial during the early stages of insect vector attacks on trees (Mageroy et al. 2020). Conversely, although *O. bicolor* is not attractive to *I. typographus* (Kandasamy et al. 2019; Zhao et al. 2019), *I. nitidus* prefers to feed on *O. bicolor*-colonised substrates and may benefit from their aid in detoxification and improved ecological fitness (Wang et al. 2023). The mechanisms underlying the functional diversity traits in *O. bicolor* and their roles in tree–beetle–fungal interactions need to be further explored.

Table 3. Strains of ophiostomatalean fungi associated with *Polygraphus* in this study.

Taxon	Genus	Species group and complex	Species	Numbers of isolates[1]					Total	Total Percentages
				PrJ	PrY	PrZ	PpZ	PpQ		
1	*Grosmannia*	*G. penicillata*	*G. crassifolia*				8		8	1.81%
2			*G. maixiuensis*				9		9	2.04%
3			*Grosmannia* sp. 1			10		2	12	2.71%
4	*Leptographium*	*L. lundbergii*	*L. griffithii*		14				14	3.17%
5			*L. jilongense*	1					1	0.23%
6			*L. pseudojilongense*	3					3	0.68%
7			*L. yadongense*		77				77	17.42%
8		*L. olivaceum*	*L. breviscapum*				33		33	7.47%
9	*Ophiostoma*	*O. clavatum*	*O. pseudobrevipilosi*		59				59	13.35%
10			*O. stebbingi*	16					16	3.62%
11			*Ophiostoma* sp. 1	18					18	4.07%
12		*O. ips*	*O. bicolor*				20	60	80	18.10%
13			*O. shigatsense*	4					4	0.90%
14		Group A	*O. maixiuense*	28	39		25		92	20.81%
15			*O. pacis*				1		1	0.23%
16			*O. sanum*			15			15	3.39%
Total				70	189	25	96	62	442	100.00%

[1] PrJ = *Polygraphus rudis* from Jilong County; PrY = *P. rudis* from Yadong County; PrZ = *P. rudis* from Zeku County; PpZ = *P. poligraphus* from Zeku County; PpQ = *P. poligraphus* from Qilian County.

Comparisons of the fungal assemblages of bark beetles from the north-eastern and southern Qinghai-Tibet Plateau showed different patterns (30 vs. 12 fungal species), with only *O. maixiuense* being a shared species (Suppl. material 1: tables S2, S3), which may be due to biogeographic barriers and host species. On the north-eastern Qinghai-Tibet Plateau, there are 14, 21 and 14 fungal associates of *Dendroctonus*, *Ips* and *Polygraphus*, respectively (Yin et al. 2016, 2019, 2020; Chang et al. 2020; Wang et al. 2021, 2024). *Ophiostoma ainoae*, *O. bicolor*, *O. nitidum*, *O. sanum* and *O. shangrilae* are shared by these three beetle genera, the latter three of which are currently found only on the Qinghai-Tibet Plateau, whereas the first two are thought to be widely distributed in the coniferous forests of China and are associated with a variety of bark beetles (Chang et al. 2019; Wang et al. 2024). Six fungal associates of *Polygraphus* were shared only with *Ips* and only two were shared with *Dendroctonus* (Suppl. material 1: table S2). This may be because of overlap in the niches of the first two genera of beetles. Furthermore, *Dendroctonus* mainly harms trunks below the DBH (diameter at breast height) of the host tree, which is not the preferred choice for *Polygraphus* and *Ips*. On the southern Qinghai-Tibet Plateau, although the straight-line distance between Jilong and Yadong Counties is not large, the fungal assemblages of bark beetles from the two Counties are divergent, with only one of the 12 species shared (Suppl. material 1: table S3). Interestingly, the fungal associations of different beetles at the two sites were highly coincident. Four of the six fungal associates of *P. rudis* are shared with *I. stebbingi*. Similarly, all four of the *P. rudis*' fungal associates in Yadong County were also isolated from *I. schmutzenhoferi* by Wang et al. (2024). This suggests that the biogeographic barrier caused by the high mountain-and-gorge landform on the southern slopes of the Himalayas creates this fungal assemblage pattern of bark beetles, even though the host species are the same and geographical distances are not far.

Overall, this study deepens our understanding of the composition of ophiostomatoid fungi associated with bark beetles, especially *Polygraphus*, on the Qinghai-Tibet Plateau. The discovery of a large number of new fungal species and new tree-bark beetle-fungal associations has made it an urgent task to reveal their biological functions and ecological features.

Additional information

Conflict of interest

The authors have declared that no competing interests exist.

Ethical statement

No ethical statement was reported.

Funding

This work was supported by the National Natural Science Foundation of China [32301598] and the National Key R&D Program of China [2023YFC2604801-4].

Author contributions

Conceptualization, Zheng Wang, Quan Lu; data curation, Zheng Wang, Caixia Liu, Xiuyue Song, Yingjie Tie; funding acquisition, Zheng Wang; investigation, Zheng Wang, Caixia Liu, Huimin Wang, Quan Lu; project administration, Zheng Wang; resources, Zheng

Wang, Caixia Liu, Xiuyue Song, Yingjie Tie; supervision, Zheng Wang, Huixiang Liu, Quan Lu; writing-original draft, Zheng Wang; writing-review and editing, Zheng Wang, Quan Lu. All authors have read and agreed to the published version of the manuscript.

Author ORCIDs

Zheng Wang https://orcid.org/0000-0003-0207-4321
Quan Lu https://orcid.org/0000-0002-6007-2677

Data availability

All of the data that support the findings of this study are available in the main text or Supplementary Information.

References

Alamouti SM, Kim JJ, Humble LM, Uzunovic A, Breuil C (2007) Ophiostomatoid fungi associated with the northern spruce engraver, *Ips perturbatus*, in western Canada. Antonie van Leeuwenhoek 91(1): 19–34. https://doi.org/10.1007/s10482-006-9092-8

Bentz BJ, Jönsson AM (2015) Modeling bark beetle responses to climate change. In: Vega FE, Hofstetter RW (Eds) Bark Beetles Biology and Ecology of Native and Invasive Species. London: Elsevier, Academic Press, 533–553 pp.

Biedermann PH, Müller J, Grégoire JC, Gruppe A, Hagge J, Hammerbacher A, Hofstetter RW, Kandasamy D, Kolarik M, Kostovcik M, Krokene P, Sallé A, Six DL, Turrini T, Vanderpool D, Wingfield MJ, Bässler C (2019) Bark beetle population dynamics in the Anthropocene: Challenges and solutions. Trends in Ecology & Evolution 34(10): 914–924. https://doi.org/10.1016/j.tree.2019.06.002

Chang R, Duong TA, Taerum SJ, Wingfield MJ, Zhou X, De Beer ZW (2017) Ophiostomatoid fungi associated with conifer-infesting beetles and their phoretic mites in Yunnan, China. MycoKeys 28: 19–64. https://doi.org/10.3897/mycokeys.28.21758

Chang R, Duong TA, Taerum SJ, Wingfield MJ, Zhou X, Yin M, De Beer ZW (2019) Ophiostomatoid fungi associated with the spruce bark beetle *Ips typographus*, including 11 new species from China. Persoonia 42(1): 50–74. https://doi.org/10.3767/persoonia.2019.42.03

Chang R, Duong TA, Taerum SJ, Wingfield MJ, Zhou X, De Beer ZW (2020) Ophiostomatoid fungi associated with mites phoretic on bark beetles in Qinghai, China. IMA Fungus 11(1): 1–18. https://doi.org/10.1186/s43008-020-00037-9

Darriba D, Taboada GL, Doallo R, Posada D (2012) jModelTest 2: More models, new heuristics and parallel computing. Nature Methods 9(8): 772–772. https://doi.org/10.1038/nmeth.2109

De Beer ZW, Wingfield MJ (2013) Emerging lineages in the Ophiostomatales. In: Seifert KA, De Beer ZW, Wingfield MJ (Eds) The Ophiostomatoid fungi: expanding frontiers, CBA biodiversity series. Netherlands: CBS-KNAW Fungal Biodiversity Centre, 21–46 pp.

De Beer ZW, Seifert KA, Wingfield MJ (2013) The ophiostomatoid fungi: their dual position in the Sordariomycetes. In: Seifert KA, De Beer ZW, Wingfield MJ (Eds) The Ophiostomatoid fungi: expanding frontiers, CBA biodiversity series. Netherlands: CBS-KNAW Fungal Biodiversity Centre, 19 pp.

De Beer ZW, Duong TA, Wingfield MJ (2016) The divorce of *Sporothrix* and *Ophiostoma*: Solution to a problematic relationship. Studies in Mycology 83(1): 165–191. https://doi.org/10.1016/j.simyco.2016.07.001

De Beer ZW, Procter M, Wingfield MJ, Marincowitz S, Duong TA (2022) Generic boundaries in the Ophiostomatales reconsidered and revised. Studies in Mycology 101(1): 57–120. https://doi.org/10.3114/sim.2022.101.02

Fortier CE, Musso AE, Evenden ML, Zaharia LI, Cooke JE (2024) Evidence that Ophiostomatoid fungal symbionts of mountain pine beetle do not play a role in overcoming lodgepole pine defenses during mass attack. Molecular Plant-Microbe Interactions 37(5): 445–458. https://doi.org/10.1094/MPMI-06-23-0077-R

Gardes M, Bruns TD (1993) ITS primers with enhanced specificity for basidiomycetes-application to the identification of mycorrhizae and rusts. Molecular Ecology 2(2): 113–118. https://doi.org/10.1111/j.1365-294X.1993.tb00005.x

Glass NL, Donaldson GC (1995) Development of primer sets designed for use with the PCR to amplify conserved genes from filamentous ascomycetes. Applied and Environmental Microbiology 61(4): 1323–1330. https://doi.org/10.1128/aem.61.4.1323-1330.1995

Huang FS, Lu J (2015) The Classification Outline of Scolytidae from China. Shanghai: Tongji University Press, 37–38 pp.

Jacobs K, Bergdahl DR, Wingfield MJ, Halik S, Seifert KA, Bright DE, Wingfield BD (2004) *Leptographium wingfieldii* introduced into North America and found associated with exotic *Tomicus piniperda* and native bark beetles. Mycological Research 108(4): 411–418. https://doi.org/10.1017/S0953756204009748

Kandasamy D, Gershenzon J, Andersson MN, Hammerbacher A (2019) Volatile organic compounds influence the interaction of the Eurasian spruce bark beetle (*Ips typographus*) with its fungal symbionts. The ISME Journal 13(7): 1788–1800. https://doi.org/10.1038/s41396-019-0390-3

Kandasamy D, Zaman R, Nakamura Y, Zhao T, Hartmann H, Andersson MN, Hammerbacher A, Gershenzon J (2023) Conifer-killing bark beetles locate fungal symbionts by detecting volatile fungal metabolites of host tree resin monoterpenes. PLoS Biology 21(2): e3001887. https://doi.org/10.1371/journal.pbio.3001887

Katoh K, Rozewicki J, Yamada KD (2019) MAFFT online service: Multiple sequence alignment, interactive sequence choice and visualization. Briefings in Bioinformatics 20(4): 1160–1166. https://doi.org/10.1093/bib/bbx108

Kirisits T (2004) Fungal associates of European bark beetles with special emphasis on the ophiostomatoid fungi. In: Lieutier F, Day KR, Battisti A, Gregoire JC, Evans HF (Eds) Bark and Wood Boring Insects in Living Trees in Europe. London: Kluwer Academic Publishers, 185–223 pp.

Kumar S, Stecher G, Tamura K (2016) MEGA7: Molecular evolutionary genetics analysis version 7.0 for bigger datasets. Molecular Biology and Evolution 33(7): 1870–1874. https://doi.org/10.1093/molbev/msw054

Lesk C, Coffel E, D'Amato AW, Dodds K, Horton R (2017) Threats to North American forests from southern pine beetle with warming winters. Nature Climate Change 7(10): 713–717. https://doi.org/10.1038/nclimate3375

Liu Y, Zhou Q, Wang Z, Wang H, Zheng G, Zhao J, Lu Q (2022) Pathophysiology and transcriptomic analysis of *Picea koraiensis* inoculated by bark beetle-vectored fungus *Ophiostoma bicolor*. Frontiers in Plant Science 13: 944336. https://doi.org/10.3389/fpls.2022.944336

Mageroy MH, Christiansen E, Långström B, Borg-Karlson AK, Solheim H, Björklund N, Zhao T, Schmidt A, Fossdal CG, Krokene P (2020) Priming of inducible defenses protects Norway spruce against tree-killing bark beetles. Plant, Cell & Environment 43(2): 420–430. https://doi.org/10.1111/pce.13661

Netherer S, Kandasamy D, Jirosová A, Kalinová B, Schebeck M, Schlyter F (2021) Interactions among Norway spruce, the bark beetle *Ips typographus* and its fungal

symbionts in times of drought. Journal of Pest Science 94(3): 591–614. https://doi.org/10.1007/s10340-021-01341-y

O'Donnell K, Cigelnik E (1997) Two divergent intragenomic rDNA ITS2 types within a monophyletic lineage of the fungus *Fusarium* are nonorthologous. Molecular Phylogenetics and Evolution 7(1): 103–116. https://doi.org/10.1006/mpev.1996.0376

Papek E, Ritzer E, Biedermann PH, Cognato AI, Baier P, Hoch G, Kirisits T, Schebeck M (2024) The pine bark beetle *Ips acuminatus*: An ecological perspective on life-history traits promoting outbreaks. Journal of Pest Science 97(3): 1–30. https://doi.org/10.1007/s10340-024-01765-2

Popkin G (2021) Forest fight. Science 374(6572): 1184–1189. https://doi.org/10.1126/science.acx9733

Raffa KF, Gregoire JC, Lindgren BS (2015) Natural history and ecology of bark beetles. In: Vega FE, W HR (Eds) Bark Beetles: Biology and Ecology of Native and Invasive Species. Elsevier, San Diego, 40 pp. https://doi.org/10.1016/B978-0-12-417156-5.00001-0

Ronquist F, Huelsenbeck JP (2003) MrBayes 3: Bayesian phylogenetic inference under mixed models. Bioinformatics 19(12): 1572–1574. https://doi.org/10.1093/bioinformatics/btg180

Solheim H (1988) Pathogenicity of some *Ips typographus*-associated blue-stain fungi to Norway spruce. Medd Nor Inst Skoforsk 40: 1–11.

Stamatakis A (2014) RAxML version 8: A tool for phylogenetic analysis and post-analysis of large phylogenies. Bioinformatics 30(9): 1312–1313. https://doi.org/10.1093/bioinformatics/btu033

Sydow H, and Sydow P (1919) Mycologische Mitteilungen. Annales Mycologici 17: 33e47.

Viklund L, Rahmani R, Bång J, Schroeder M, Hedenström E (2019) Optimizing the attractiveness of pheromone baits used for trap** the four-eyed spruce bark beetle *Polygraphus poligraphus*. Journal of Applied Entomology 143(7): 721–730. https://doi.org/10.1111/jen.12641

Vilgalys R, Hester M (1990) Rapid genetic identification and mapping of enzymatically amplified ribosomal DNA from several *Cryptococcus* species. Journal of Bacteriology 172(8): 4238–4246. https://doi.org/10.1128/jb.172.8.4238-4246.1990

Wadke N, Kandasamy D, Vogel H, Lah L, Wingfield BD, Paetz C, Wright LP, Gershenzon J, Hammerbacher A (2016) The bark-beetle-associated fungus, *Endoconidiophora polonica*, utilizes the phenolic defense compounds of its host as a carbon source. Plant Physiol. 171(2):914–931. https://doi.org/10.1104/pp.15.01916

Wang Z, Liu Y, Wang H, Meng X, Liu X, Decock C, Zhang X, Lu Q (2020) Ophiostomatoid fungi associated with *Ips subelongatus*, including eight new species from northeastern China. IMA Fungus 11(1): 3. https://doi.org/10.1186/s43008-019-0025-3

Wang Z, Zhou Q, Zheng G, Fang J, Han F, Zhang X, Lu Q (2021) Abundance and diversity of ophiostomatoid fungi associated with the Great Spruce Bark Beetle (*Dendroctonus micans*) in the Northeastern Qinghai-Tibet Plateau. Frontiers in Microbiology 12: 721395. https://doi.org/10.3389/fmicb.2021.721395

Wang Z, Liu Y, Wang H, Roy A, Liu H, Han F, Zhang X, Lu Q (2023) Genome and transcriptome of *Ips nitidus* provide insights into high-altitude hypoxia adaptation and symbiosis. iScience 26(10): 107793. https://doi.org/10.1016/j.isci.2023.107793

Wang Z, Liang L, Wang H, Decock C, Lu Q (2024) Ophiostomatoid fungi associated with *Ips* bark beetles in China. PREPRINT (Version 1) [available at Research Square]. https://doi.org/10.21203/rs.3.rs-4896600/v1

White TJ, Bruns T, Lee S, Taylor J (1990) Amplification and direct sequencing of fungal ribosomal RNA genes for phylogenetics. PCR Protocols: A Guide to Methods and Applications 18: 315–322. https://doi.org/10.1016/B978-0-12-372180-8. 50042-1

Yamaoka Y, Wingfield MJ, Takahashi I, Solheim H (1997) Ophiostomatoid fungi associated with the spruce bark beetle *Ips typographus* f. *japonicus* in Japan. Mycological Research 101(10): 1215–1227. https://doi.org/10.1017/S0953756297003924

Yin HF, Huang FS, Li ZL (1984) Economic Insect Fauna of China (Fasc. 29) Coleoptera: Scolytidae. Beijing: Science Press, 82–92 pp.

Yin M, Wingfield MJ, Zhou X, De Beer ZW (2016) Multigene phylogenies and morphological characterization of five new *Ophiostoma* spp. associated with spruce-infesting bark beetles in China. Fungal Biology 120(4): 454–470. https://doi.org/10.1016/j.funbio.2015.12.004

Yin M, Wingfield MJ, Zhou X, Linnakoski R, De Beer ZW (2019) Taxonomy and phylogeny of the *Leptographium olivaceum* complex (Ophiostomatales, Ascomycota), including descriptions of six new species from China and Europe. MycoKeys 60: 93–123. https://doi.org/10.3897/mycokeys.60.39069

Yin M, Wingfield MJ, Zhou X, De Beer ZW (2020) Phylogenetic re-evaluation of the *Grosmannia penicillata* complex (Ascomycota, Ophiostomatales), with the description of five new species from China and USA. Fungal Biology 124(2): 110–124. https://doi.org/10.1016/j.funbio.2019.12.003

Zhao T, Axelsson K, Krokene P, Borg-Karlson AK (2015) Fungal symbionts of the spruce bark beetle synthesize the beetle aggregation pheromone 2-methyl-3-buten-2-ol. Journal of Chemical Ecology 41(9): 848–852. https://doi.org/10.1007/s10886-015-0617-3

Zhao T, Ganji S, Schiebe C, Bohman B, Weinstein P, Krokene P, Borg-Karlson AK, Unelius CR (2019) Convergent evolution of semiochemicals across Kingdoms: Bark beetles and their fungal symbionts. The ISME Journal 13(6): 1535–1545. https://doi.org/10.1038/s41396-019-0370-7

Zipfel RD, De Beer ZW, Jacobs K, Wingfield BD, Wingfield MJ (2006) Multi-gene phylogenies define *Ceratocystiopsis* and *Grosmannia* distinct from *Ophiostoma*. Studies in Mycology 55(1): 75–97. https://doi.org/10.3114/sim.55.1.75

Supplementary material 1

Supplementary tables

Authors: Zheng Wang, Caixia Liu, Xiuyue Song, Yingjie Tie, Huimin Wang, Huixiang Liu, Quan Lu

Data type: rar

Explanation note: **table S1.** List of sampling information of *Polygraphus* bark beetles. **table S2.** Comparisons of fungal assemblages of bark beetles in the north-eastern Qinghai-Tibet Plateau. **table S3.** Comparisons of fungal assemblages of bark beetles in the southern Qinghai-Tibet Plateau.

Link: https://doi.org/10.3897/mycokeys.110.135538.suppl1

Supplementary material 2

Supplementary figures

Authors: Zheng Wang, Caixia Liu, Xiuyue Song, Yingjie Tie, Huimin Wang, Huixiang Liu, Quan Lu

Data type: rar

Explanation note: **figure S1.** Phylogram of *Grosmannia penicillata* complex (including Taxa 1–3) based on *tub2* sequence data. **figure S2.** Phylogram of *Grosmannia penicillata* complex (including Taxa 1–3) based on *tef1-α* sequence data. **figure S3.** Phylogram of *Leptographium lundbergii* complex (including Taxa 4–7) based on *tub2* sequence data. **figure S4.** Phylogram of *Leptographium lundbergii* complex (including Taxa 4–7) based on *tef1-α* sequence data. **figure S5.** Phylogram of *Leptographium olivaceum* complex (including Taxon 8) based on *tub2* sequence data. **figure S6.** Phylogram of *Leptographium olivaceum* complex (including Taxon 8) based on *tef1-α* sequence data. **figure S7.** Phylogram of *Ophiostoma clavatum* complex (including Taxa 9–11) based on *tub2* sequence data. **figure S8.** Phylogram of *Ophiostoma clavatum* complex (including Taxa 9–11) based on *tef1-α* sequence data. **figure S9.** Phylogram of Group A (including Taxa 14–16) based on ITS sequence data. The ML bootstrap support values ≥ 70% and posterior probability values ≥ 0.9 are recorded at the nodes. T = ex-type isolates. **figure S10.** Phylogram of Group A (including Taxa 14–16) based on *tub2* sequence data.

Link: https://doi.org/10.3897/mycokeys.110.135538.suppl2